

# Study of stacking faults in Co-alloy perpendicular media

Bin Lu, Timothy Klemmer, Kurt Wierman, Ganping Ju, and Dieter Weller  
*Seagate Technology, 2403 Sidney Street, Ste 550, Pittsburgh, Pennsylvania 15203*

Anup G. Roy and David E. Laughlin  
*Data Storage System Center, Carnegie Mellon University, Pittsburgh, Pennsylvania 15213*

Chunghee Chang and Rajiv Ranjan  
*Seagate Technology, 47010 Kato Road, Fremont, California 94538*

Stacking faults (SFs) and fcc-phased grains are studied by electron diffraction in perpendicular media. Co-alloy compositions, such as CoCrPt, CoCrPtB, are compared on different underlayers and deposition conditions. It is found that CoCrPtB alloys tend to have greater amount of SFs and fcc grains than the CoCrPt alloy. Underlayers as well as low deposition rate and base pressure help to reduce the amount of SFs and fcc phase. © 2002 American Institute of Physics.

[DOI: 10.1063/1.1452269]

## I. INTRODUCTION

High perpendicular anisotropy is critical for obtaining adequate thermal stability in future ultrahigh density magnetic recording media.<sup>1</sup> For Co-alloys, in order to achieve high  $K_u$  as well as an adequate ratio of anisotropy and demagnetization fields ( $H_k/4\pi M_s \sim 2-3$ ), it is important to reduce the amount of fcc grains and stacking faults (SFs).<sup>2</sup> However, in pursuing the perfect preferred orientation, the control of hetero-epitaxy is different between longitudinal and perpendicular media. Figure 1 illustrates the difference in a schematic diagram. In the longitudinal case, there is a good match between Co hcp-(11.0) lattice plane and Cr (200) plane, while there is a poor lattice match between the corresponding Co fcc-(112) plane and Cr (200) plane. Therefore, it is much more favorable for hcp Co structure to grow at the interface.

On the other hand, in the perpendicular media case, the lattice match is always good between the underlayer [e.g., Ru (00.2)] and the magnetic layer, Co hcp-(00.2) or Co fcc-(111). Consequently, no constraint is available through the entire film to limit the fcc growth. Under these considerations, it can be predicted that there will be more fcc and SFs in the perpendicular media than in the longitudinal media. Moreover, it can also be expected that alloy compositions that work well for longitudinal media may not work for perpendicular media. For example, it has been found<sup>3</sup> that perpendicular media of CoCrPtB alloy have lower remanence and lower  $H_k$  compared to the respective longitudinal media<sup>4</sup> with same composition.

In addition, SF detection in longitudinal media is established based on x-ray diffraction,<sup>5</sup> transmission electron microscopy<sup>6</sup> and electron diffraction.<sup>7</sup> These techniques need to be re-visited for perpendicular media. In this work the amount of fcc grains and SF density in perpendicular media is studied by electron diffraction (ED). The purpose of this study is not only to demonstrate an ED method qualitatively studying the SFs and fcc grains in perpendicular media, but also to understand the role of alloy composition, deposition

rate and underlayer on the SF density and number of fcc grains in the perpendicular media.

## II. EXPERIMENT

CoCrPtB and CoCrPt thin films were dc-sputter deposited onto glass substrates (or Si wafers) with (or without) underlayers at elevated temperature. FeCoB is used as the soft magnetic underlayers (SUL).<sup>8</sup> The intermediate layer (IL) is similar to the one described in Ref. 9. The deposition was carried out by using an Intevac MDP sputter system at a deposition rate of 4 nm/s. One CoCrPtB sample was made in a K. J. Lesker UHV sputter system at lower base pressure ( $10^{-10}$  Torr) and much slower deposition rate (0.35 nm/s). A homemade PMOKE looper was utilized to obtain hysteresis loops. A Philips EM420 TEM was used for electron diffraction with a double tilt specimen holder.

## III. RESULTS AND DISCUSSION

The geometric setting of the crystal structures in perpendicular media is different from longitudinal media. In the former, all the  $c$ -axes of Co-alloys are parallel to the film normal, while in the latter, the  $c$ -axes are randomly oriented in the film plane. Accordingly, the fcc grains can be randomly oriented in a longitudinal film, where the SF-caused

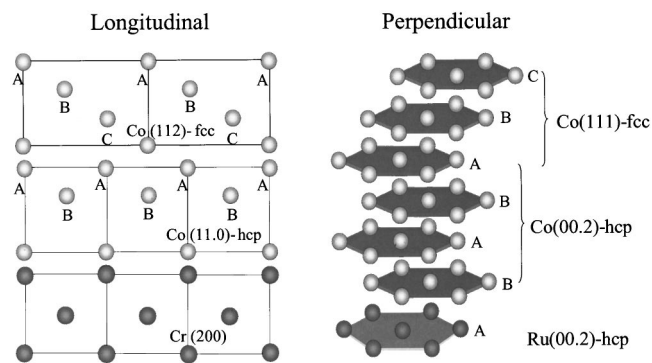


FIG. 1. Schematic diagram of the epitaxial relationships in longitudinal (left) and perpendicular media (right).

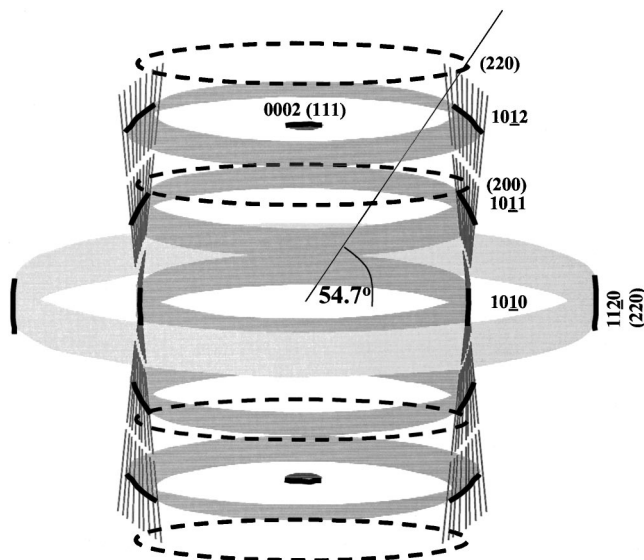


FIG. 2. Schematic diagram of the reciprocal structure of a perpendicular media with stacking faults and fcc grains.

ED streaks, which should always be parallel to the  $c$ -axis, lie randomly in the film plane.<sup>7</sup> In contrast, in the perpendicular media, the fcc grains are most likely (111) textured<sup>10</sup> and the SF streaks are parallel to the film normal. This difference in crystallographic configuration requires a different procedure to detect fcc grains and SFs in perpendicular media. Figure 2 shows a schematic diagram of the reciprocal structure of the Co-alloy film in a side-view. The hcp phases are plotted in dark bands, while the position of fcc reciprocal rings are marked by broken lines and indexed within the parentheses. The SF streaks and diffraction arcs of the hcp phase are plotted only at the cross-section plane, which contributes to a cross-sectional ED pattern. However, the major difficulty of the cross-sectional ED is the small amount of material participating in the ED and difficulty in preparing the specimen. Plan-view ED can overcome these two drawbacks by tiling the specimen to a high angle (e.g.,  $54.7^\circ$  as marked in the Fig. 2). Under these tilted conditions one can see the SF-streak intersections with Ewald sphere as well as fcc (220) diffraction arcs (if present).

Five perpendicular media samples of different layer structures as described in Table I are investigated. The normalized MOKE hysteresis loops of samples A–D are plotted in Fig. 3. It can be seen that without any underlayers the Co-alloy film (sample A) has extremely low remanence and coercivity ( $H_c$ ). The CoCrPtB films of samples B, C and E have low remanence and moderate coercivities, compared

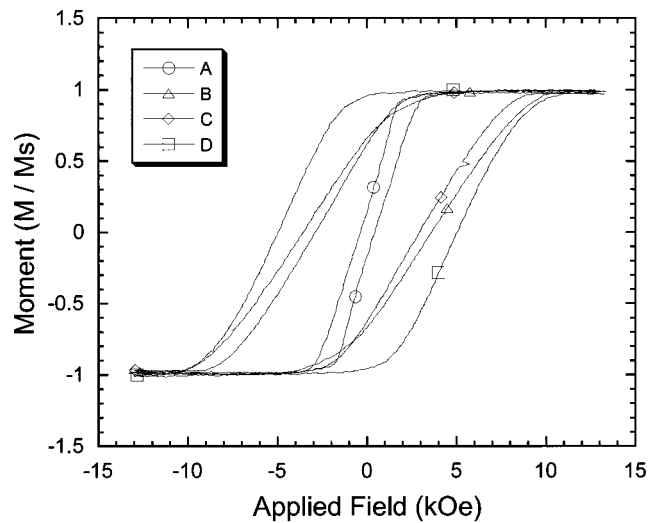


FIG. 3. Normalized hysteresis loops of samples A, B, C, and D.

with their longitudinal-media equivalents.<sup>4</sup> On the other hand the CoCrPt media have the highest  $H_c$  and almost full remanence.

$50^\circ$ -tilt ED patterns of the samples A–E are shown in Figs. 4(a)–4(e), respectively. Figure 4(f) is the schematic diagram of the diffraction rings that may possibly be present in a perpendicular Co-alloy thin film. The dotted rings belong to the fcc phase and are indexed within parentheses. In Fig. 4(a) the presence of the 11.0 arc along the tilt axis indicates a (00.2) crystallographic texture of the Co-alloy film. In addition, there are two arcs at the same radial position as the 11.0 arc but perpendicular to the tilt axis. These cannot belong to the hcp phase, which has a uni-axial crystal structure. They originate from fcc 220 reflections in a (111) texture. Moreover, the arcs in the ED pattern are almost continuous, forming a whole ring, which indicates a weak hcp-(00.2)/fcc-(111) texture. There are many cloudy dots (pointed to by the arrow) between the first wide ring and the second ring. These dots are due to the SF streaks from 10.2 and 10.3 arcs intersecting with the Ewald sphere. Therefore, it can be concluded that the Co-alloy film that is directly deposited onto a glass substrate has poor crystallographic texture, and large amount of fcc grains and SFs.

In the ED pattern of Fig. 4(b) the rings break into arcs indicating a stronger texture than found in sample A. However, the hcp-11.0 and fcc-220 arcs still stay at the same ring position perpendicular to each other, though the fcc-220 arcs bear lower intensity than the ones in Fig. 4(a). In the position where 10.2, 10.3 arcs are present [refer to the indexed arc

TABLE I. Samples of the perpendicular Co-alloy thin films for the electron diffraction study.

ID	Substrate	SUL thickness	IL thickness	Magnetic layer	$H_c$ (Oe)	$S$
A	Glass	0	0	CoCrPtB <sub>10</sub> (20 nm)	349	0.13
B	Glass	200 nm	10 nm	CoCrPtB <sub>10</sub> (24 nm)	3575	0.67
C	Glass	200 nm	10 nm	CoCrPtB <sub>12</sub> (24 nm)	2914	0.62
D	Glass	200 nm	10 nm	CoCrPt (24 nm)	4985	0.96
E	Si-wafer	0	30 nm	CoCrPtB <sub>6</sub> (40 nm)	3000	0.57

